Research Article

Cancer Prevention Research

Telomere Shortening Alters the Kinetics of the DNA Damage Response after Ionizing Radiation in Human Cells

Rachid Drissi[1], Jing Wu[2], Yafang Hu[3], Carol Bockhold[2], and Jeffrey S. Dome[3]

Abstract

Studies of telomerase-deficient mice and human cell lines have showed that telomere shortening enhances sensitivity to ionizing radiation (IR). The molecular basis for this observation remains unclear. To better understand the connection between telomere shortening and radiation sensitivity, we evaluated components of the DNA damage response pathway in normal human fibroblasts with short and long telomeres. Late-passage cells with short telomeres showed enhanced sensitivity to IR compared with early-passage cells with longer telomeres. Compared with early-passage cells, late-passage cells had a higher baseline level of phosphorylated H2AX protein (γH2AX) before IR but diminished peak levels of H2AX phosphorylation after treatment with IR. Both the appearance and disappearance of γH2AX foci were delayed in late-passage cells, indicative of delayed DNA repair. In contrast to the situation with H2AX, ATM and p53 phosphorylation kinetics were similar in early- and late-passage cells, but phosphorylation of the chromatin-bound ATM targets SMC1 and NBS1 was delayed in late-passage cells. Because impaired phosphorylation associated with short telomeres was restricted to chromatin-bound ATM targets, chromatin structure was assessed. DNA from cells with short telomeres was more resistant to digestion with micrococcal nuclease, indicative of compacted chromatin. Moreover, cells with short telomeres showed histone acetylation and methylation profiles consistent with heterochromatin. Together our data suggest a model in which short telomeres induce chromatin structure changes that limit access of activated ATM to its downstream targets on the chromatin, thereby providing a potential explanation for the increased radiation sensitivity seen with telomere shortening.
Cancer Prev Res; 4(12); 1973–81. *©2011 AACR.*

Introduction

There has been growing recognition of a close relationship between telomeres and the DNA damage response (1). Proteins involved in the DNA damage response localize to telomeres and are required for normal telomere maintenance yet are also involved in the cellular response to telomere shortening and dysfunction (2). Cells with short or dysfunctional telomeres activate a damage response similar to the response observed with DNA double-strand breaks, including activation of ATM, phosphorylation of ATM targets, and formation of nuclear foci containing protein complexes involved in DNA repair (3–5). The telomere-induced damage response arises, in part, from direct uncapping of telomeres and is not solely attributed to end-to-end fusions of dysfunctional telomeres leading to chromosome breakage during anaphase.

The link between telomeres and the DNA damage response has been furthered by several studies, both at cellular and organismal levels, showing that telomere shortening and dysfunction are determinants of radiation sensitivity (6–11). However, the molecular basis underlying this sensitivity remains unclear. Understanding how telomere integrity influences sensitivity to DNA-damaging agents is especially relevant, given the emergence of telomerase inhibition as a therapeutic modality for human cancers. In the present study, we compared the cellular response to ionizing radiation (IR) in isogenic human cells with short and long telomeres. Our data show that the kinetics of the DNA damage response is altered in cells with short telomeres and suggest that telomere shortening is associated with chromatin structure changes that limit access of activated ATM to its chromatin-bound downstream targets.

Authors' Affiliations: [1]Division of Oncology, Cincinnati Children's Hospital Medical Center, Cincinnati, Ohio; [2]Department of Oncology, St. Jude Children's Research Hospital, Memphis, Tennessee; and [3]Division of Oncology, Children's National Medical Center, Washington, District of Columbia

Note: Supplementary data for this article are available at Cancer Prevention Research Online (http://cancerprevres.aacrjournals.org/).

Corresponding Authors: Jeffrey S. Dome, Division of Oncology, Children's National Medical Center, 111 Michigan Avenue NW, Washington, DC 20010. Phone: 202-476-3656; Fax: 1-202-476-5648; E-mail: jdome@cnmc.org; and Rachid Drissi, Division of Oncology, Cincinnati Children's Hospital Medical Center, MLC 7013, 3333 Burnet Avenue, Cincinnati, OH 45229. Phone: 513-803-0674; Fax: 513-636-2880; E-mail: rachid.drissi@cchmc.org

doi: 10.1158/1940-6207.CAPR-11-0069

©2011 American Association for Cancer Research.

Materials and Methods

Cell culture

The ATCC CRL-2091 normal primary human foreskin fibroblast strain (HFF) and the HeLa human cervical carcinoma cell line were obtained from the American Type Culture Collection. 293T cells were a gift from Dr. David Baltimore; no authentication of 293T cells was done by the authors. Cells were propagated in Dulbecco's Modified Eagle's Media (Biowhittaker) supplemented with 10% FBS (HyClone), L-Glutamine, and penicillin/streptomycin (Gibco) at 37°C and 5% CO_2 in a humidified incubator. Fibroblasts were trypsinized and counted every 7 days and reseeded at a density of 5×10^5 cells per 75 cm^2 flask. HeLa cells were counted every 3 to 4 days and replated at a density of 0.5×10^6 to 1×10^6 cells per 100 mm dish. The histone deacetylase (HDAC) inhibitor vorinostat (LC laboratories) was dissolved in dimethyl sulfoxide and applied to cells at a concentration of 2 μmol/L. Cells were treated with vorinostat for 24 hours prior to irradiation.

Generation of TERT constructs and retroviruses

Plasmids containing human TERT cDNA (pCI-neo-hEST2) were a gift from Dr. Robert Weinberg (Whitehead Institute for Biomedical Research, Cambridge, MA). Catalytically inactive TERT-dominant negative (TERT-DN) was generated by substituting the aspartic acid residues with valine residues at positions 868 and 869 by site-directed mutagenesis (Quick Change Site-directed Mutagenesis kit; Stratagene). The TERT and TERT-DN mutants were sequenced completely and subcloned into the retroviral expression vector MSCV-IGFP, which expresses the GFP reporter from an internal ribosomal entry site (IRES). Vesicular stomatitis virus-G (VSV-G)-pseudotyped retroviruses were packaged in 293T cells transfected with the plasmids pEQ-PAM3-E (containing the helper proteins), VSV-G (containing the envelope), and MSCV-IGFP, MSCV-IGFP-TERT, or MSCV-IGFP-TERT-DN. Virus-containing medium was applied to the cells of interest in 3 separate aliquots with polybrene, as previously described (12). Forty-eight hours after transduction, GFP-containing cells were isolated by fluorescence-activated cell sorting (FACS). The experiments described were carried out on HFFs taken in the early passages after transduction with the hTERT retrovirus when a sufficient number of cells were available after FACS sorting (estimated to be several population doublings). HeLa cells transduced with the mutant TERT-DN constructs were cloned by the limiting dilution method. The process of generating visible HeLa cell colonies required 20 population doublings.

Telomerase activity and telomere length assays

Cell extracts were prepared according to protocols provided by the manufacturers. Telomerase activity was measured using the TRAPeze Telomerase Detection Kit (Intergen). For telomere length analysis, 5 μg genomic DNA was digested with *Hin*fI and *Rsa*I and analyzed by southern blotting using ^{32}P-labeled $(TTAGGG)_6$ probe. Signals were visualized using a PhosphorImager (Storm 860, Molecular Dynamics).

Clonogenic survival assays

Cells were seeded onto 6-well plates in concentrations predicted to yield 100 to 200 colonies per well. Increasing cell concentrations were used for increasing doses of IR. For the IR experiments, cells were subjected to the indicated doses of IR 20 hours after seeding. Two weeks after irradiation, the cells were fixed and stained with 0.01% formaldehyde and 0.1% crystal violet. Colonies containing at least 50 cells were counted.

Immunoprecipitation, Western blotting, and immunofluorescence

All procedures are described in the works of Bakkenist and colleagues (3) and Kitagawa and colleagues (13). Briefly, cells extracts were prepared in radioimmunoprecipitation assay (RIPA) buffer (200 mmol/L NaCl, 10 mmol/L Tris at pH 7.5, 0.1% SDS, 1% NP-40, 0.5% deoxycholate, 1× protease inhibitor cocktail tablet from Roche), anti-SMC1 (BL308; Bethyl Laboratories), anti-SMC1S957-P, anti-p53 (Ab-6; Oncogene Research Products), anti-p53S15-P (Cell Signaling Technology), anti-β-actin (Novus Biologicals), anti-acetyl-Histone H3K9 (Upstate), anti-dimethyl-Histone H3K9 (Upstate), anti-H3, CT, pan, clone A3S (Upstate), anti-γH2AX (Millipore), anti-NBS1 (Novus Biologicals), and anti-NBS1S343-P (Signalway Antibody).

Histone extraction

Extracts containing soluble histone proteins were prepared as described previously (13). In brief, cell pellets were resuspended in hypotonic buffer (10 mmol/L HEPES at pH = 7.9, 1.5 mmol/L $MgCl_2$, and 10 mmol/L KCl). Cells were then lysed in a hypertonic lysis buffer (10 mmol/L HEPES at pH = 7.9, 1.5 mmol/L $MgCl_2$, 250 mmol/L NaCl, 10 mmol/L KCl, 0.2 mol/L HCl, 0.5 mmol/L DTT, 1.5 mmol/L phenylmethylsulfonylfluoride, and 1× protease inhibitor cocktail tablet from Roche). Cell extracts were dialyzed against 0.1 mol/L acetic acid twice for 1 hour and 3 times against H_2O for 1 hour, 3 hours, and overnight, respectively.

Micrococcal nuclease assay

Cells were permeabilized for 90 seconds with 0.01% egg-Lysolecithin (Sigma) diluted in 150 mmol/L sucrose, 80 mmol/L KCl, 35 mmol/L HEPES, pH = 7.4, 5 mmol/L K_2HPO_4, 5 mmol/L $MgCl_2$, and 0.5 mmol/L $CaCl_2$. Cells were then digested with 2 U/mL micrococcal nuclease (Sigma) in 20 mmol/L sucrose, 50 mmol/L Tris-HCl, pH = 7.5, 50 mmol/L NaCl, and 2 mmol/L $CaCl_2$ at room temperature for various time points. DNA was isolated and subjected to 6% PAGE to analyze the digestion products.

Results

Cells with short telomeres are more sensitive to IR

To evaluate the sensitivity of cells with short telomeres to IR, we used clonogenic survival assays at different

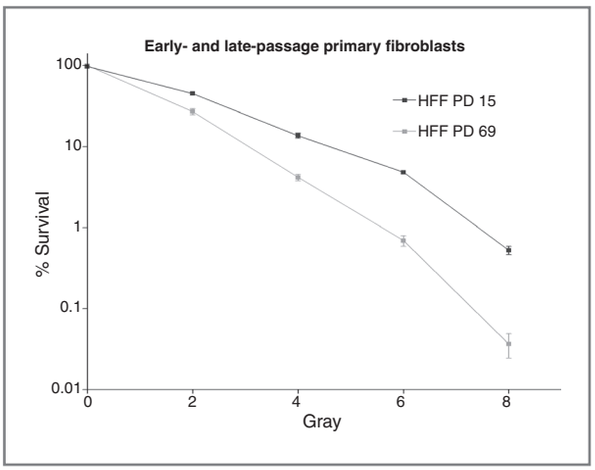

Figure 1. Cells with short telomeres are more sensitive to IR. Early- (PD 15) and late-passage (PD 69) HFFs were irradiated at the indicated IR doses. The surviving fraction of cells was determined using a clonogenic survival assay.

population doublings of primary HFFs. We previously had shown that telomeres shorten in HFFs at each population doubling (3). Late-passage fibroblasts with short telomeres had significantly enhanced sensitivity to IR compared with early-passage fibroblasts (Fig. 1). To confirm that IR sensitivity is associated with short telomeres, we also introduced a catalytically inactive dominant-negative hTERT construct (hTERT-DN) to inhibit telomerase activity in HeLa cells. Transduced cells were cloned by the limiting dilution method. Sensitivity to IR was assessed at different population doublings using clonogenic survival assays. The introduction of hTERT-DN into HeLa cells resulted in complete inhibition of detectable telomerase activity (Supplementary Fig. S1A) and telomere shortening with successive population doublings (PD; Supplementary Fig. S1B). Cells with short telomeres were markedly more sensitive to IR than their counterparts with longer telomeres (Supplementary Fig. S1C).

Kinetics of γH2AX nuclear focus formation and resolution are delayed in cells with short telomeres

Cellular survival following DNA damage depends on the integrity of the signaling pathways to repair DNA double-strand breaks (DSB) and restore genomic integrity. H2AX phosphorylation is an early step in the response to DNA damage. Upon irradiation, H2AX is rapidly phosphorylated by activated ATM and DNA protein kinases (DNA-PK) on serine 139 to generate γH2AX, a robust marker of DSBs (14, 15) that can be used to monitor DSB repair (16). Both activated ATM and γH2AX form nuclear foci upon DSBs. The extent of DNA damage post-irradiation and the kinetics of γH2AX foci formation and resolution were evaluated in late- and early-passage HFFs by immunofluorescence using γH2AX-S139 phospho-specific antibodies. Late-passage cells were presenescent, as evidenced by continued growth and lack of senescence-associated β-galactosidase staining (Supplemental Fig. S2). Although the cells were presenescent, they were growing at a slower rate than early-passage cells. To control for differences in cell growth, most of the experiments outlined below were carried out on contact-inhibited cells that were 3 weeks past the point of confluence.

As expected, at baseline before subjecting cells to IR, late-passage (PD 63) HFF cultures had a higher percentage of cells with γH2AX foci than early-passage cultures (PD 11). However, upon irradiation, a higher peak percentage of early-passage HFFs manifested γH2AX foci than late-passage HFFs (Fig. 2A). Moreover, the kinetics of γH2AX foci appearance and disappearance was faster in early-passage than late-passage HFFs (Fig. 2A and B). Similar results were obtained using Western blot analysis to assess γH2AX protein levels (Fig. 2C). Thirty minutes after 1 Gy of IR, early-passage HFFs showed a robust induction of H2AX phosphorylation, whereas late-passage HFFs did not increase γH2AX protein levels until 60 minutes after IR (Fig. 2C, lanes 3 and 4). At 5 hours post-irradiation, while γH2AX protein levels were still elevated in late-passage HFFs, γH2AX protein levels returned to near baseline levels in early-passage HFFs (Fig. 2C, lanes 9 and 10). γH2AX foci disappeared at later time point in late-passage cells, 16 hours post-irradiation (Fig. 2C, lanes 15 and 16).

Effect of ectopic hTERT expression on γH2AX foci formation and resolution

To confirm that the altered kinetics of DNA repair observed in late-passage HFF was telomere dependent, we transduced HFFs at late passage (PD 64) with a retroviral vector that expresses hTERT. Transduced cells exhibited telomerase activity and elongated telomeres in early passages after the cells were harvested after the transduction (Supplementary Fig. S3). Ectopic telomerase expression in late-passage cells completely restored the kinetics of γH2AX foci formation and resolution to the levels observed with early-passage cells (Fig. 3A), showing that telomere dysfunction, rather than other effects of prolonged cell culture such as oxidative damage, was responsible for the altered H2AX phosphorylation. Similar results were obtained using Western blot analysis to assess γH2AX protein levels (Fig. 3B).

ATM, p53, SMC1, and NBS1 phosphorylation in early- and late-passage HFFs

To further characterize the delayed DNA repair kinetics observed in late-passage HFFs, we assessed other members of the DNA damage response pathway. ATM is rapidly activated in response to DSBs and phosphorylates key proteins leading to cell-cycle arrest, senescence, and apoptosis (17). ATM substrates include p53, NBS1, H2AX, 53BP1, BRCA1, SMC1, and Chk2 (18, 19). Because late-passage cells showed delayed H2AX phosphorylation and γH2AX foci formation, we surmised that ATM activation may also be delayed. To test this hypothesis, the kinetics of ATM activation (measured by ATM-S1981P) after

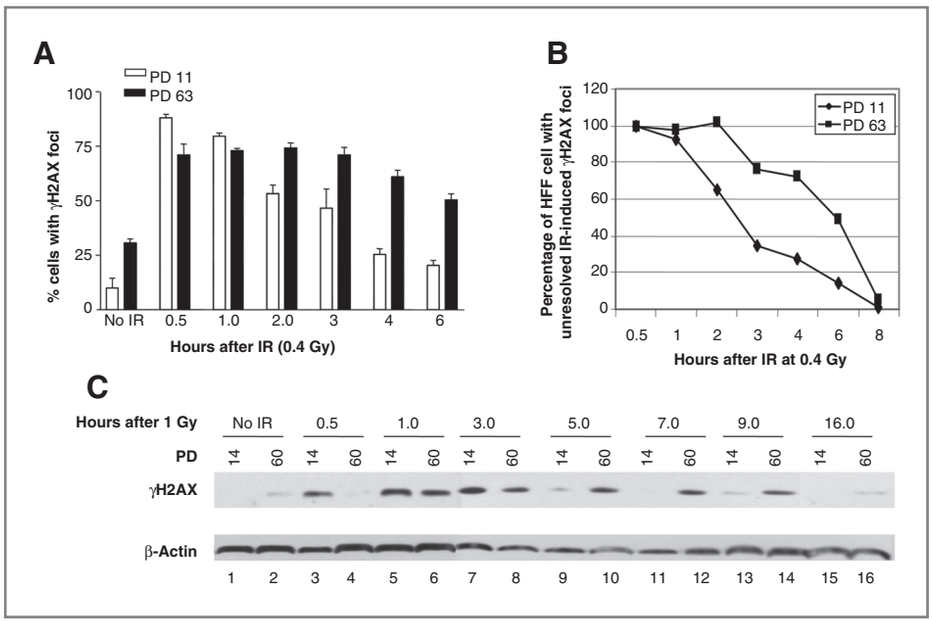

Figure 2. Kinetics of γH2AX foci formation and resolution are delayed in cells with short telomeres. A, early- (PD 11) and late-passage (PD 63) HFFs were irradiated with 0.4 Gy and processed for immunofluorescence using anti-γH2AX antibodies at the indicated time post-irradiation. A total of 100 cells were analyzed, cells with 3 or more foci were considered γH2AX positive. B, time course of γH2AX resolution, the percentage of cells with unresolved γH2AX IR-induced foci was assessed in early- and late-passage at the indicated time following irradiation with 0.4 Gy. C, early- and late-passage HFFs were irradiated with 1 Gy and harvested at the indicated time points post-irradiation for histone protein extraction. Phosphorylated H2AX protein levels were assessed using anti-γH2AX antibodies.

irradiation was evaluated in early- and late-passage HFFs that were contact inhibited for several weeks. Similar to the observation with H2AX, late-passage HFFs had a higher baseline level of ATM activation than early-passage cells. However, in contrast to the situation with H2AX phosphorylation, there was no striking difference in the level of ATM activation between early- and late-passage HFFs in response to IR (Fig. 4A). Moreover, the kinetics of ATM-S1981P nuclear focus formation was similar in early- and late-passage cells (Fig. 4B). We also evaluated the phosphorylation of p53, SMC1, and NBS1 in early- and late-passage HFFs. The accumulation of p53 protein and its phosphorylation on S15 occurred with the same kinetics after irradiation in early- and late-passage cells (Fig. 4C). However, the phosphorylation of SMC1 on S957 and NBS1 on S343 was delayed in late-passage cells (Fig. 4C and D). Together these results suggest that late-passage cells exhibit a delay in phosphorylation of ATM target proteins bound to chromatin such as H2AX, SMC1, and NBS1. Proteins that are not chromatin bound, such as p53 and ATM itself, have similar

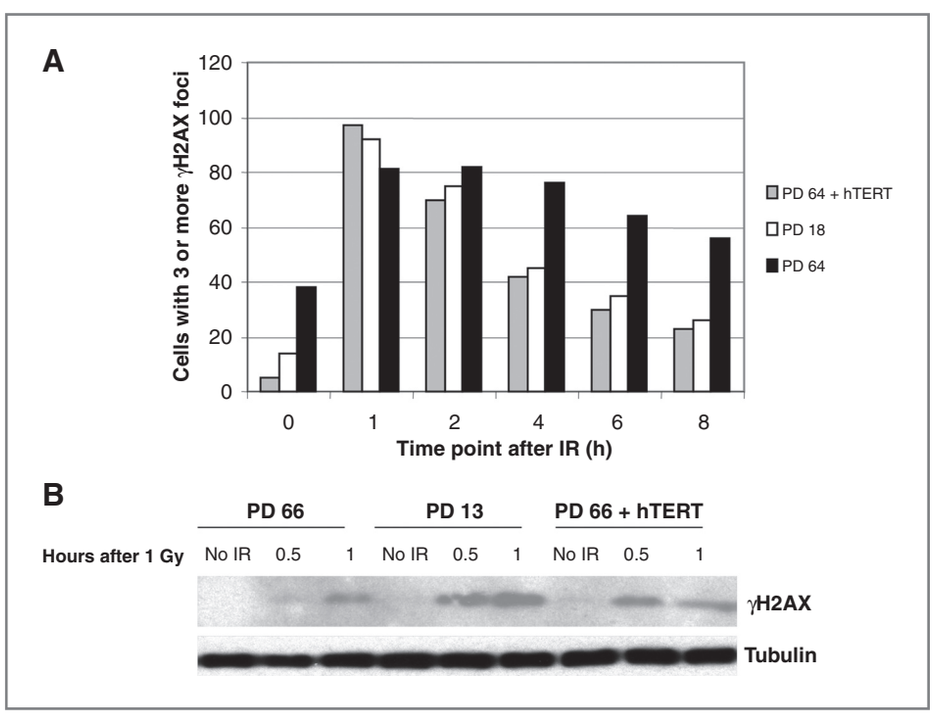

Figure 3. Delayed kinetics of γH2AX foci formation and resolution are suppressed by ectopic hTERT expression. A, early- and late-passage HFFs transduced with an hTERT-expressing retrovirus vector were irradiated with 0.4 Gy and analyzed by immunofluorescence with anti-γH2AX at the indicated time points post-irradiation. Cells were considered positive if 3 or more foci were present. B, kinetics of H2AX phosphorylation after 1 Gy IR was assessed by immunoblot with anti-γH2AX in early- and late-passage cells transduced with the hTERT retrovirus.

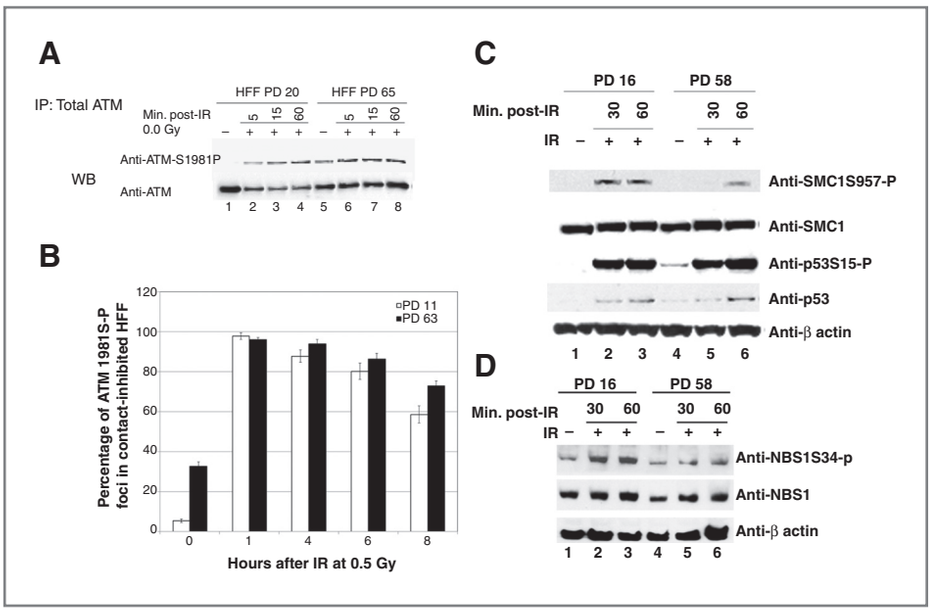

Figure 4. Delayed phosphorylation kinetics of chromatin-bound proteins. A, ATM phosphorylation kinetics post-irradiation is similar in early- and late-passage HFFs. HFFs at PD 20 and 65 were irradiated with 0.2 Gy. Cells were harvested at the indicated time points post-irradiation and whole-cell extracts were prepared. Cleared supernatants were immunoprecipitated (IP) with anti-ATM, and the samples were resolved by gel electrophoresis and immunoblotted with anti-total ATM and anti-ATM 1981S-P. B, kinetics of ATM1981S-P foci formation is similar in early- and late-passage HFFs. HFFs at PD 11 and 63 were irradiated with 0.5 Gy and the kinetics of ATMS1981-P foci formation was assessed at the indicated time points post-irradiation. A total of 100 cells per time point were analyzed, cells with 3 or more foci were considered ATMS1981-P positive. The values shown are the mean ± SD of 5 fields analyzed of 100 cells each. C and D, HFFs at PD 16 and 58 were irradiated with 10 Gy and harvested at the indicated time points for immunoblotting. Total and phosphorylated p53 SMC1 and NBS1 were assessed. WB, Western blot.

levels of activation in response to IR in late- and early-passage cells.

Changes in chromatin structure are associated with short telomeres

The delay in phosphorylation of H2AX, SMC1, and NBS1 might be induced by chromatin structure change, triggered by short telomeres, resulting in limited access of activated ATM to its chromatin-bound downstream targets. To test this hypothesis, we used the micrococcal nuclease assay to analyze chromatin structure in late- and early-passage cells. Consistent with the resistance of compacted chromatin to limited nuclease digestion (20), at an early time point (1 minute), chromatin from late-passage presenescent cells was more resistant to micrococcal nuclease digestion than early-passage cells, suggesting that late-passage chromatin is compacted (Fig. 5A and B). The resistance to micrococcal nuclease was completely abolished in late-passage cells expressing hTERT, linking this resistance to telomere dysfunction.

Chromatin from late-passage cells has features of heterochromatin

To determine whether late-passage compacted chromatin is related to heterochromatin, we examined H3K9 acetylation and methylation levels. Consistent with the features seen with compact chromatin (21), our results indicated reduced levels of H3 acetyl K9 and increased levels of H3 dimethyl K9 in late-passage cells (Fig. 6, lanes 1 and 3). Ectopic expression of hTERT in late-passage cells reversed H3K9 acetylation and methylation profiles, suggesting that these histone modifications are caused by short telomeres (Fig. 5, lane 4). Moreover, this reversal required an active hTERT on telomeres, as the ectopic expression of hTERT-DN or hTERT-HA (a form of hTERT that is catalytically active but unable to elongate telomeres and prevent senescence; ref. 22) did not reverse these profiles (Fig. 6, lanes 5 and 6).

To further assess whether chromatin state was responsible for the diminished DNA damage response in late-passage cells, we treated late-passage HFFs with the HDAC inhibitor vorinostat, which promotes histone acetylation and an open chromatin state. Treatment with the HDAC inhibitor restored the intensity and rapidity of H2AX phosphorylation in late-passage cells (Fig. 6B). Together, these results suggest a model in which short telomeres induce chromatin structure change consistent with heterochromatin, causing chromatin compaction and limited access of ATM kinase to its chromatin targets, thereby potentially contributing to enhanced radiosensitivity in late-passage cells.

Discussion

In the present study, we evaluated the mechanism of enhanced radiosensitivity in cells with short telomeres. As expected, primary and transformed cells with short telomeres had markedly enhanced sensitivity to IR compared

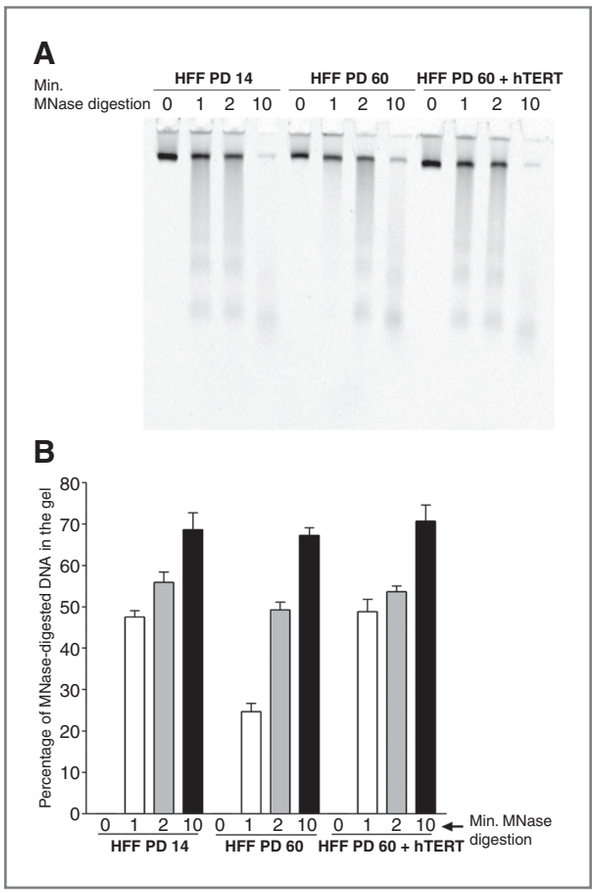

Figure 5. Compaction of chromatin structure in late-passage cells is reversed by hTERT ectopic expression. A, resistance of late-passage cells to micrococcal nuclease digestion. Micrococcal nuclease digestion of permeabilized HFF cells at PD 14, 60, and 60 transduced with retrovirus expressing hTERT. DNA was isolated from cells after micrococcal digestion for the indicated time in minutes and resolved by PAGE. B, quantification of the DNA amounts in (A) entering the gel relative to undigested DNA at 0 minutes. The values shown are the mean ± SD of 3 independent experiments.

with cells with longer telomeres. These results mirror the results observed in *Terc* knockout mice, which showed that progressive telomere shortening was associated with enhanced cellular and organismal sensitivity to IR (7, 11). Similar results have been observed in human cells (23–26). Although some studies have suggested that telomerase expression *per se* influences radiosensitivity (8, 27), our results and the results of other groups suggest that telomere length is the primary determinant of radiosensitivity (7, 11, 25, 28, 29, 30). In these studies, ectopic telomerase expression or telomerase inhibition had no effect on sensitivity to IR until a measurable change in telomere length was observed.

The biological mechanism underlying the relationship between telomere integrity and radiation sensitivity remains to be determined. A simple model to explain this correlation is that cells with short telomeres possess a baseline level of DNA damage from uncapped telomeres even before they are subjected to IR. In this model, the preexisting damage would be additive with the extra damage induced by IR, thereby enhancing radiation sensitivity. Arguing against this model is our observation that the baseline number of γH2AX foci in late-passage fibroblasts is equivalent to an IR dose of only 0.1 Gy (data not shown). Adding 0.1 Gy to the levels of IR that were used in the clonogenic survival assays would be insufficient to explain the enhanced sensitivity to IR that we observed, though the protracted 0.1-Gy equivalent exposure in late-passage cells may be biologically different from the short-lived exposure associated with a one-time dose of IR. Although the baseline number of γH2AX foci in late-passage cells was elevated compared with early-passage HFFs, the late-passage cells had diminished H2AX phosphorylation in response to IR at early time points (Fig. 2). If the enhanced radiation sensitivity in late-passage cells was merely the result of an additive effect of radiation damage to telomere damage, we would have expected the peak levels of H2AX phosphorylation to be higher in the late-passage cells than the early-passage cells. A second model that has been proposed is that telomeres serve as repositories of proteins that participate in the DNA damage response, which can readily translocate to DNA breaks (11). According to this premise, once telomeres become short, repair proteins can no longer bind telomeres and are no longer immediately available to sites of DNA damage. However, the DSB repair proteins that associate with telomeres, such as the MRE11/RAD50/NBS1 (MRN) complex, are uniformly distributed in the nuclei of unirradiated cells (31). Because the telomere-bound component comprises just a small fraction of the abundant pool of repair proteins, it seems unlikely that a decrease in telomere length would have a major effect on the availability of repair proteins to be recruited to DNA breaks.

The present data support a third model for increased radiation sensitivity in cells with short telomeres. One of the earliest events in the DNA damage response is ATM phosphorylation/activation and swift phosphorylation of H2AX (γH2AX) on serine 139, primarily by activated ATM and DNA-PK (15, 18). Upon DSB, phosphorylated H2AX (γH2AX) rapidly forms DNA repair foci that include the MRN complex, 53BP1, and BRCA1 (32). Our results showed that late-passage cells had attenuated peak levels of H2AX phosphorylation and that the kinetics of H2AX phosphorylation and dephosphorylation were delayed. Because γH2AX plays a crucial role in the recruitment of proteins to the repair focus and in its stabilization to recruit late factors, such as cohesions, to tether sister chromatids for homologous recombination repair pathway (33–36), the altered H2AX phosphorylation kinetics may account for the enhanced radiosensitivity in late-passage cells. Recently, it was shown that telomerase-null and telomerase-inhibited mouse embryo fibroblasts (MEF) formed fewer γH2AX foci and had delayed appearance and disappearance of such foci following heat shock and IR exposure compared with telomerase-positive MEFs (6). Although these results focused on telomerase expression and not telomere length, they are concordant with our results. Furthermore, delayed

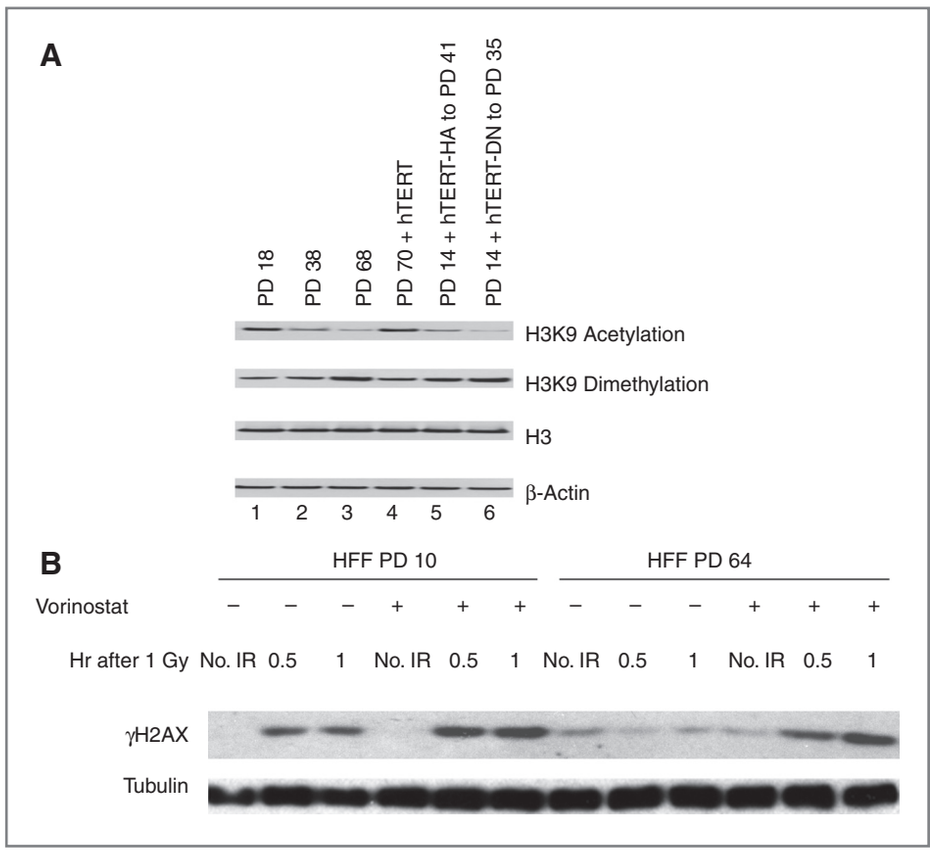

Figure 6. Reduced H3K9 acetylation and increased methylation levels in cells with short telomeres. A, HFFs at the indicated PD numbers were processed for acid cellular extraction of histone proteins (see Materials and Methods), lysates were analyzed by immunoblotting with anti-acetyl-Histone H3K9, anti-dimethyl-Histone H3K9, and anti-H3. HFFs at PD 14 were transduced with retrovirus expressing hTERT hemagglutinin (HA) tagged at C-terminal and passaged to PD 41 after transduction. HA-hTERT was shown to have *in vitro* telomerase enzymatic activity but did not maintain telomeres (22). HFFs at PD 14 were transduced with retrovirus expressing an hTERT-DN and passaged to PD 35. B, cells were treated with 2 μmol/L of the HDAC inhibitor vorinostat prior to irradiation. After 1 Gy IR, H2AX protein was extracted and assessed for phosphorylation by immunoblotting with anti-γH2AX.

kinetics of DNA DSB processing, including the rates of recruitment of DSB repair proteins to γH2AX foci, has been observed in normal and pathologic aging (9).

Our data suggest a mechanism for the altered kinetics of γH2AX foci formation and disappearance in late-passage cells. Late-passage chromatin was resistant to micrococcal nuclease digestion and had reduced levels of H3K9 acetylation and higher levels H3K9 dimethylation, indicative of heterochromatinization. These results are consistent with the observation that senescent cells accumulate foci of heterochromatin (37), though the late-passage fibroblasts used in our experiments were presenescent (Supplementary Fig. S2). The compacted chromatin could explain why phosphorylation and activation of chromatin-bound DNA damage proteins (H2AX, SMC1, and NBS1) were delayed in late-passage cells, whereas activation of non–chromatin-bound proteins (p53 and ATM) was unchanged. Moreover, we observed that dephosphorylation of γH2AX was delayed in late-passage cells. Dephosphorylation of γH2AX is achieved by protein phosphatase 2A (38), by the HTP-C phosphatase complex in budding yeast (39) and by Wip1 phosphatase (40–42). Like delayed phosphorylation of chromatin-bound proteins, delayed dephosphorylation may be caused by reduced access of phosphatases to late-passage chromatin. Furthermore, we and others have shown that H3K9Ac is a DNA damage–responsive modification [Zhang and Drissi, unpublished data; ref. (43)], suggesting that this histone modification is a mark of heterochromatin and DNA damage.

Telomerase protein has also been described to regulate chromatin state and the DNA damage response (27). Suppression of hTERT in human fibroblasts led to enhanced radiosensitivity and delayed kinetics of γH2AX foci formation, without measurable changes in telomere length. Abrogation of hTERT was associated with a pattern of euchromatin (enhanced sensitivity to micrococcal nuclease–induced DNA digestion, increased H3K9 acetylation, and decreased H3K9 dimethylation). It is interesting that although the end result of telomerase suppression (enhanced radiosensitivity and delayed DNA repair kinetics) was similar to the effect we observed with telomere shortening, telomerase suppression increased euchromatin content whereas telomere shortening increased heterochromatin content. These results indicate that although telomerase repression and telomere shortening are closely intertwined, the two processes do not have identical consequences for the cell.

It remains to be determined how telomere length influences chromatin structure and, in turn, how chromatin structure influences the DNA repair process. It has recently been shown that ATM-mediated phosphorylation of heterochromatin-promoting proteins, such as KAP-1, increases the repair of DNA breaks within heterochromatin (44). Our data showed that ATM activation kinetics in late-passage

cells was not affected by short telomeres but that phosphorylation of H2AX, SMC1, and NBS1 was delayed. It is possible that telomere shortening–induced heterochromatin introduces an impediment to ATM-dependent chromatin modifications that facilitate DNA DSB repair.

Finally, our results support several predictions about the use of telomerase inhibitors as therapeutic agents for human cancer. First, telomerase inhibition in itself can induce apoptosis and growth arrest in cancer cells, though this response may be delayed, as observed in our HeLa cells. Second, the concurrent administration of telomerase inhibitors and IR may have a synergistic effect once sufficient telomere shortening has occurred. The concurrent application of DNA-damaging agents and telomerase inhibitors may provide a therapeutic benefit.

Disclosure of Potential Conflicts of Interest

No potential conflicts of interest were disclosed.

Grant Support

The research was supported by grants CA87903 and CA111347 from the NIH to J.S. Dome, the American Lebanese Syrian Associated Charities (ALSAC) of St. Jude Children's Research Hospital, and the Children's Cancer Foundation.

The costs of publication of this article were defrayed in part by the payment of page charges. This article must therefore be hereby marked *advertisement* in accordance with 18 U.S.C. Section 1734 solely to indicate this fact.

Received February 2, 2011; revised August 11, 2011; accepted September 8, 2011; published OnlineFirst September 19, 2011.

References

1. de Lange T. Telomere biology and DNA repair: enemies with benefits. FEBS Lett 2010;584:3673–4.
2. Palm W, de Lange T. How shelterin protects mammalian telomeres. Annu Rev Genet 2008;42:301–34.
3. Bakkenist CJ, Drissi R, Wu J, Kastan MB, Dome JS. Disappearance of the telomere dysfunction-induced stress response in fully senescent cells. Cancer Res 2004;64:3748–52.
4. d'Adda di Fagagna F, Reaper PM, Clay-Farrace L, Fiegler H, Carr P, Von Zglinicki T, et al. A DNA damage checkpoint response in telomere-initiated senescence. Nature 2003;426:194–8.
5. Takai H, Smogorzewska A, de Lange T. DNA damage foci at dysfunctional telomeres. Curr Biol 2003;13:1549–56.
6. Agarwal M, Pandita S, Hunt CR, Gupta A, Yue X, Khan S, et al. Inhibition of telomerase activity enhances hyperthermia-mediated radiosensitization. Cancer Res 2008;68:3370–8.
7. Goytisolo FA, Samper E, Martin-Caballero J, Finnon P, Herrera E, Flores JM, et al. Short telomeres result in organismal hypersensitivity to ionizing radiation in mammals. J Exp Med 2000;192:1625–36.
8. Nakamura M, Masutomi K, Kyo S, Hashimoto M, Maida Y, Kanaya T, et al. Efficient inhibition of human telomerase reverse transcriptase expression by RNA interference sensitizes cancer cells to ionizing radiation and chemotherapy. Hum Gene Ther 2005;16:859–68.
9. Sedelnikova OA, Horikawa I, Redon C, Nakamura A, Zimonjic DB, Popescu NC, et al. Delayed kinetics of DNA double-strand break processing in normal and pathological aging. Aging Cell 2008;7:89–100.
10. Wesbuer S, Lanvers-Kaminsky C, Duran-Seuberth I, Bolling T, Schafer KL, Braun Y, et al. Association of telomerase activity with radio- and chemosensitivity of neuroblastomas. Radiat Oncol 2010;5:66.
11. Wong KK, Chang S, Weiler SR, Ganesan S, Chaudhuri J, Zhu C, et al. Telomere dysfunction impairs DNA repair and enhances sensitivity to ionizing radiation. Nat Genet 2000;26:85–8.
12. Zindy F, Eischen CM, Randle DH, Kamijo T, Cleveland JL, Sherr CJ, et al. Myc signaling via the ARF tumor suppressor regulates p53-dependent apoptosis and immortalization. Genes Dev 1998;12:2424–33.
13. Kitagawa R, Bakkenist CJ, McKinnon PJ, Kastan MB. Phosphorylation of SMC1 is a critical downstream event in the ATM-NBS1-BRCA1 pathway. Genes Dev 2004;18:1423–38.
14. Rogakou EP, Boon C, Redon C, Bonner WM. Megabase chromatin domains involved in DNA double-strand breaks *in vivo*. J Cell Biol 1999;146:905–16.
15. Stiff T, O'Driscoll M, Rief N, Iwabuchi K, Lobrich M, Jeggo PA. ATM and DNA-PK function redundantly to phosphorylate H2AX after exposure to ionizing radiation. Cancer Res 2004;64:2390–6.
16. Rothkamm K, Lobrich M. Evidence for a lack of DNA double-strand break repair in human cells exposed to very low x-ray doses. Proc Natl Acad Sci U S A 2003;100:5057–62.
17. Kastan MB, Bartek J. Cell-cycle checkpoints and cancer. Nature 2004;432:316–23.
18. Bakkenist CJ, Kastan MB. DNA damage activates ATM through intermolecular autophosphorylation and dimer dissociation. Nature 2003;421:499–506.
19. Shiloh Y, Kastan MB. ATM: genome stability, neuronal development, and cancer cross paths. Adv Cancer Res 2001;83:209–54.
20. Leuba SH, Zlatanova J, van Holde K. On the location of linker DNA in the chromatin fiber. Studies with immobilized and soluble micrococcal nuclease. J Mol Biol 1994;235:871–80.
21. Grewal SI, Rice JC. Regulation of heterochromatin by histone methylation and small RNAs. Curr Opin Cell Biol 2004;16:230–8.
22. Counter CM, Hahn WC, Wei W, Caddle SD, Beijersbergen RL, Lansdorp PM, et al. Dissociation among *in vitro* telomerase activity, telomere maintenance, and cellular immortalization. Proc Natl Acad Sci U S A 1998;95:14723–8.
23. Hauguel T, Bunz F. Haploinsufficiency of hTERT leads to telomere dysfunction and radiosensitivity in human cancer cells. Cancer Biol Ther 2003;2:679–84.
24. Rubio MA, Davalos AR, Campisi J. Telomere length mediates the effects of telomerase on the cellular response to genotoxic stress. Exp Cell Res 2004;298:17–27.
25. Rubio MA, Kim SH, Campisi J. Reversible manipulation of telomerase expression and telomere length. Implications for the ionizing radiation response and replicative senescence of human cells. J Biol Chem 2002;277:28609–17.
26. Sharma GG, Hwang KK, Pandita RK, Gupta A, Dhar S, Parenteau J, et al. Human heterochromatin protein 1 isoforms HP1(Hsalpha) and HP1(Hsbeta) interfere with hTERT-telomere interactions and correlate with changes in cell growth and response to ionizing radiation. Mol Cell Biol 2003;23:8363–76.
27. Masutomi K, Possemato R, Wong JM, Currier JL, Tothova Z, Manola JB, et al. The telomerase reverse transcriptase regulates chromatin state and DNA damage responses. Proc Natl Acad Sci U S A 2005;102:8222–7.
28. Vaziri H, Squire JA, Pandita TK, Bradley G, Kuba RM, Zhang H, et al. Analysis of genomic integrity and p53-dependent G1 checkpoint in telomerase-induced extended-life-span human fibroblasts. Mol Cell Biol 1999;19:2373–9.
29. Erdmann N, Harrington LA. No attenuation of the ATM-dependent DNA damage response in murine telomerase-deficient cells. DNA Repair (Amst) 2009;8:347–53.
30. Hemann MT, Strong MA, Hao LY, Greider CW. The shortest telomere, not average telomere length, is critical for cell viability and chromosome stability. Cell 2001;107:67–77.
31. Maser RS, Mirzoeva OK, Wells J, Olivares H, Williams BR, Zinkel RA, et al. Mre11 complex and DNA replication: linkage to E2F and sites of DNA synthesis. Mol Cell Biol 2001;21:6006–16.

32. Paull TT, Rogakou EP, Yamazaki V, Kirchgessner CU, Gellert M, Bonner WM. A critical role for histone H2AX in recruitment of repair factors to nuclear foci after DNA damage. Curr Biol 2000;10: 886–95.

33. Celeste A, Fernandez-Capetillo O, Kruhlak MJ, Pilch DR, Staudt DW, Lee A, et al. Histone H2AX phosphorylation is dispensable for the initial recognition of DNA breaks. Nat Cell Biol 2003;5: 675–9.

34. Strom L, Lindroos HB, Shirahige K, Sjogren C. Postreplicative recruitment of cohesin to double-strand breaks is required for DNA repair. Mol Cell 2004;16:1003–15.

35. Unal E, Arbel-Eden A, Sattler U, Shroff R, Lichten M, Haber JE, et al. DNA damage response pathway uses histone modification to assemble a double-strand break-specific cohesin domain. Mol Cell 2004; 16:991–1002.

36. Xie A, Puget N, Shim I, Odate S, Jarzyna I, Bassing CH, et al. Control of sister chromatid recombination by histone H2AX. Mol Cell 2004;16: 1017–25.

37. Narita M, Nunez S, Heard E, Lin AW, Hearn SA, Spector DL, et al. Rb-mediated heterochromatin formation and silencing of E2F target genes during cellular senescence. Cell 2003;113:703–16.

38. Chowdhury D, Keogh MC, Ishii H, Peterson CL, Buratowski S, Lieberman J. gamma-H2AX dephosphorylation by protein phosphatase 2A facilitates DNA double-strand break repair. Mol Cell 2005;20:801–9.

39. Keogh MC, Kim JA, Downey M, Fillingham J, Chowdhury D, Harrison JC, et al. A phosphatase complex that dephosphorylates gamma H2AX regulates DNA damage checkpoint recovery. Nature 2006;439: 497–501.

40. Cha H, Lowe JM, Li H, Lee JS, Belova GI, Bulavin DV, et al. Wip1 directly dephosphorylates gamma-H2AX and attenuates the DNA damage response. Cancer Res 2010;70:4112–22.

41. Macurek L, Lindqvist A, Voets O, Kool J, Vos HR, Medema RH. Wip1 phosphatase is associated with chromatin and dephosphorylates gammaH2AX to promote checkpoint inhibition. Oncogene 2010;29: 2281–91.

42. Moon SH, Nguyen TA, Darlington Y, Lu X, Donehower LA. Dephosphorylation of gammaH2AX by WIP1: an important homeostatic regulatory event in DNA repair and cell cycle control. Cell Cycle 2010;9: 2092–6.

43. Tjeertes JV, Miller KM, Jackson SP. Screen for DNA-damage-responsive histone modifications identifies H3K9Ac and H3K56Ac in human cells. EMBO J 2009;28:1878–89.

44. Goodarzi AA, Noon AT, Deckbar D, Ziv Y, Shiloh Y, Lobrich M, et al. ATM signaling facilitates repair of DNA double-strand breaks associated with heterochromatin. Mol Cell 2008;31:167–77.